New Journal of Physics
The open-access journal for physics

Experimentally generating and tuning robust entanglement between photonic qubits

B P Lanyon[1,3] **and N K Langford**[1,2]
[1] Department of Physics and Centre for Quantum Computer Technology, University of Queensland, QLD 4072, Brisbane, Australia
[2] Faculty of Physics, University of Vienna, Boltzmanngasse 5, A-1090 Vienna, Austria
E-mail: lanyon@physics.uq.edu.au

New Journal of Physics **11** (2009) 013008 (9pp)
Received 3 September 2008
Published 7 January 2009
Online at http://www.njp.org/
doi:10.1088/1367-2630/11/1/013008

Abstract. We introduce and demonstrate a technique for generating a range of novel multi-photon entangled states. Adjusting a simple experimental parameter allows the preparation of pure states with an arbitrary level of W-class entanglement, from a fully separable state to the maximally robust W state, enabling full control over this entanglement class in our system. Furthermore, the generated states exhibit a highly symmetric entanglement distribution that we show is optimally robust against qubit loss. The ability to prepare entanglement in robust configurations is particularly relevant to many emerging quantum technologies where entanglement is a valuable resource. We achieve a high quality experimental realization for the three-photon case, including a W state fidelity of 0.90 ± 0.03. In addition, we present a new technique for characterizing quantum states in the laboratory in the form of iterative tomography.

Large multipartite entangled states play a central role in many active areas of research including quantum computation, communication and metrology [1]–[3]. However, while entanglement in bipartite quantum systems is well understood, multipartite entanglement is relatively unexplored and offers a far more complex structure; there are various types of entanglement that present significant generation, manipulation and characterization challenges. There has already been much theoretical work devoted to classifying and quantifying to what degree and in which way multipartite states are entangled [4]–[7]. Recently, experimentalists have begun to achieve the level of control over quantum systems required to generate and study multipartite entanglement [8]–[11].

[3] Author to whom any correspondence should be addressed.

In this paper, we explore robust entanglement between three qubits; the simplest system in which the phenomenon can be observed. This feature is best exemplified by the well-known GHZ and W states:

$$|\mathrm{GHZ}\rangle = (|000\rangle + |111\rangle)/\sqrt{2}, \tag{1}$$

$$|\mathrm{W}\rangle = (|001\rangle + |010\rangle + |100\rangle)/\sqrt{3}. \tag{2}$$

These states are the canonical examples of the two inequivalent classes of three-qubit entanglement. Specifically, any state possessing genuinely tripartite entanglement can be converted into one, and only one of these states using stochastic local operations and classical communication (SLOCC) [4]. Entanglement in a GHZ state is maximally fragile; loss of information about any single qubit leaves the remaining two in a separable state. Conversely, entanglement in a three-qubit W state is maximally robust [4]; loss of the information in any single qubit leaves the remaining two in an entangled state. The question of entanglement robustness arises naturally in experimental situations from decoherence mechanisms involving loss of qubits or qubit information. This is an important consideration in the many applications where entanglement is a vital resource.

We generate and study the entanglement properties of novel states composed of three polarization-encoded photonic qubits, introducing and experimentally demonstrating a simple scheme for the preparation of pure states with an arbitrary amount of W-class robust entanglement. Furthermore, we show that over the entire range the entanglement remains in a configuration that is optimally robust against qubit loss. We achieve high fidelities with the expected states in all cases.

We generate photons using spontaneous parametric down conversion (SPDC), figure 1. Measurement of a four-fold coincidence between detectors D1–D4 selects, with high probability, the cases where the source emitted two pairs of photons into optical modes 1 and 2. The polarization of two photons in the same spatio-temporal mode represents a three-level quantum system, a biphotonic qutrit [12], with logical basis states: $|\mathbf{0}_3\rangle \equiv |2_\mathrm{H}, 0_\mathrm{V}\rangle$, $|\mathbf{1}_3\rangle \equiv |1_\mathrm{H}, 1_\mathrm{V}\rangle$ and $|\mathbf{2}_3\rangle \equiv |0_\mathrm{H}, 2_\mathrm{V}\rangle$. Passing the two-photon state of mode 1 through a horizontal polarizer prepares the state $|\mathbf{0}_3\rangle$, and we then create a superposition in mode a, using a half-wave plate set at an angle θ, of the form:

$$\cos^2 2\theta |\mathbf{0}_3\rangle + \sqrt{2}\cos 2\theta \sin 2\theta |\mathbf{1}_3\rangle + \sin^2 2\theta |\mathbf{2}_3\rangle. \tag{3}$$

Mode 2 is passed to a 50% beam splitter; detection of a single photon at D1 heralds the presence of a single photon in mode b, which is passed through a polarizing beam splitter to prepare a polarization qubit ($|\mathbf{0}_2\rangle \equiv |1_\mathrm{H}, 0_\mathrm{V}\rangle$, $|\mathbf{1}_2\rangle \equiv |0_\mathrm{H}, 1_\mathrm{V}\rangle$) in the logical state $|\mathbf{0}_2\rangle$. Thus a qubit and qutrit arrive simultaneously at the first 50% beam splitter in our optical circuit.

A successful coincidence measurement heralds the cases where a biphotonic qutrit exits the central splitter in mode d and splits into single photon states in modes e and f after the final 50% beam splitter. At the output of the circuit we find the following three-qubit joint state across modes c, e and f:

$$\frac{\cos^2 2\theta}{4} |\mathbf{0}_2, \mathbf{0}_2, \mathbf{0}_2\rangle + \frac{\cos 2\theta \sin 2\theta}{2} |\mathbf{1}_2, \mathbf{0}_2, \mathbf{0}_2\rangle + \frac{\sin^2 2\theta}{4} (|\mathbf{1}_2, \mathbf{1}_2, \mathbf{0}_2\rangle + |\mathbf{1}_2, \mathbf{0}_2, \mathbf{1}_2\rangle - |\mathbf{0}_2, \mathbf{1}_2, \mathbf{1}_2\rangle). \tag{4}$$

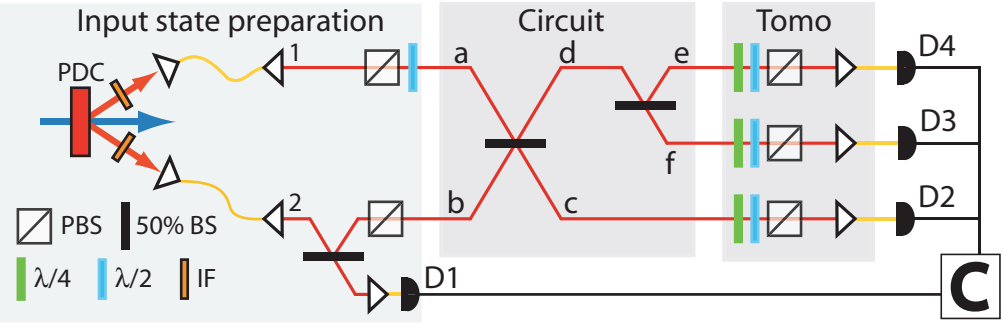

Figure 1. Conceptual experimental layout. Photons are generated via SPDC of a frequency-doubled mode-locked Ti:sapphire laser (820 nm → 410 nm, $\Delta\tau = 80$ fs at 82 MHz) through a type-I 2 mm BiB_3O_6 crystal. Photons are filtered by blocked interference filters (IF) at 820 ± 1.5 nm; collected into two single-mode optical fibres; injected into free-space modes 1 and 2; detected using fibre-coupled single photon counting modules (D1–D4). With 300 mW at 410 nm, we observe a fourfold coincidence rate of 0.1 Hz.

This is a superposition of a separable state (first two terms) and an entangled W state (last three terms). Choosing $\theta = \pi/4$ injects a biphoton in the state $|\mathbf{2}_3\rangle$ into mode a (equation (1)) and results in a three-qubit W state with probability 1/16 (equation (2)). Choosing $\theta = 0$ injects a biphoton in the state $|\mathbf{0}_3\rangle$ and produces a separable state of the form $|\mathbf{0}_2, \mathbf{0}_2, \mathbf{0}_2\rangle$.

Quantifying the amount of genuine tripartite entanglement in a three-qubit pure state is nontrivial. The three-tangle, defined as $\tau_3(\rho_{ABC}) = 4 \det\rho_A - C_{AB} - C_{BC}$, where C_{ij} is the concurrence of the reduced state ρ_{ij} [13], quantifies GHZ-class entanglement and, since it is always zero for the W class [4], can be used to distinguish the W and GHZ classes. Following the technique of [4], it is straightforward to show that our ideal output state (equation (2)) belongs to the W class for all θ[4]. An entanglement monotone useful for quantifying W-class entanglement is the tripartite negativity (N_3) [14, 15], defined as $N_3 = (N_{a(bc)} N_{b(ac)} N_{c(ab)})^{1/3}$, where the bipartite negativities are calculated using the standard definition [16]. Using this definition, the three-qubit W state has a near maximal value of $N_3 = 0.94$. Quantifying how robust the entanglement in our three-qubit system is to loss requires a measure of the residual bipartite entanglement left in the two-qubit subsystem after loss of the information contained in qubit k ($\rho_{ij} = \mathrm{Tr}_k(\rho_{ijk})$). We choose to use the tangle (τ_2) [13].

By varying θ between 0 and $\pi/4$ we are able to prepare pure states with any desired amount of W-class entanglement, thereby giving us full control over this class of entanglement in our system. This scheme can be generalized straightforwardly to generate tunable W-class entanglement for any number of qubits. Besides the fundamental interest of how to prepare multiqubit non-maximally entangled states in a given class, we note that, in the case of two qubits, such states have already found important application in fundamental tests of quantum mechanics [17]–[19]. Previous techniques for producing W states [8]–[10] do not enable this control and could not be easily modified to achieve it. Our states also possess another useful and intriguing property. It is straightforward to show that, for all θ, the residual bipartite entanglement remains symmetrically distributed between each pair of qubits,

[4] For all θ, $\tau_3 = 0$ and the state possesses nonzero bipartite entanglement in each bipartite grouping of the three-qubit subsystems.

i.e. $\tau_2(\rho_{ce})=\tau_2(\rho_{cf})=\tau_2(\rho_{fe})=4\sin^4\theta/(\cos 2\theta-2)^2$. As a result, the amount of entanglement left in a two-qubit subsystem is always independent of which qubit is lost. Later, we will show that the entanglement in these states is in fact optimally robust against qubit loss.

We measure three-qubit output states using polarization tomography [20] of modes c, e and f, performing an over-complete set of 216 separate measurements [21] in four-fold coincidence between non-photon-number-resolving detectors D1–D4. With rates of approximately $0.1\,\mathrm{s}^{-1}$, we measure for several days to acquire sufficient counts for an accurate reconstruction. Instead of performing a single measurement set over this time we take many shorter 80 min sets. This *iterative* tomography technique provides many advantages. Most importantly, a complete reconstruction of the density matrix is possible after each iteration, allowing analysis of how our estimates of state properties are developing throughout the measurement process. This allows diagnosis of serious practical problems, such as time-dependant optical misalignment, far earlier than would otherwise be possible. Using many repeated shorter measurement sets also makes the state estimation less prone to errors introduced by certain fluctuations in the optical source brightness, without significantly reducing the total available integration time. After completion we use the data accumulated across all short measurement sets to reconstruct the final state. Our experiment is neither actively stabilized nor realigned between iterative measurement sets. Our beamsplitters impart systematic unitary operations on the optical modes. While the entanglement properties of our ideal or measured states are not affected by these local operations, state fidelities are. For simplicity, we corrected for these effects numerically, but alternatively such unitaries could be corrected using standard waveplates.

Figures 2(a) and (b) show ideal and measured quantum states for $\theta=\pi/4$ (equation (2)). We find a high fidelity with the ideal W state of 0.90 ± 0.03, which violates the entanglement witness for a W state [22] by 7 standard deviations, and a high tripartite negativity of $N_3=0.80\pm0.03$. Note that we use the following standard definition for the fidelity between two mixed states: $F(\rho,\sigma)\equiv\mathrm{Tr}[\sqrt{\sqrt{\rho}\sigma\sqrt{\rho}}]^2$.

Figures 2(c) and (d) show the reduced state of qubits e and f, calculated by numerical application of a partial trace to the states in figures 2(a) and (b), respectively. We find a high fidelity of $F=0.94\pm0.02$ with the ideal maximally entangled mixed state (MEMS) [16], [23]–[25]. The tangle is $\tau_2=0.27\pm0.03$ (ideal: 4/9), demonstrating the robustness of the entanglement in the three-qubit state to loss. Figure 2(e) shows how our estimates of key properties of the generated state (figure 2(b)) developed over the iterative measurement process. The asymptotic trends show that we measured for a sufficient period of time such that our reconstructed states are a fair representation of the generated states.

Figure 3(a) shows experimental results for three-qubit states measured over a range of θ (equation (2)). We find high fidelities with the ideal symmetric robust three-qubit states (see caption). The discrepancies in the bipartite tangle seem larger than in the tripartite negativity because tangle is a harsher measure of entanglement [16]. We also measure the reduced two-qubit states *directly* by removing the polarization analysis optics from one qubit output mode at a time and only detecting its presence as a trigger—physically realizing the loss of qubit information. This was repeated for each qubit to test the symmetry of our measured states. Besides offering an unambiguous demonstration of robust entanglement, this approach offers an increased count-rate over that observed when measuring three-qubit states, allowing shorter measurement times that are less prone to experimental drift. We perform over-complete polarization tomography of the remaining two qubits using 36 measurements [29]. Figure 3(b) presents the results plotted on the tangle versus linear entropy plane [23], where the linear entropy [20] is $S_\mathrm{L}\equiv d(1-\mathrm{Tr}[\rho^2])/(d-1)$, and d is the state dimension.

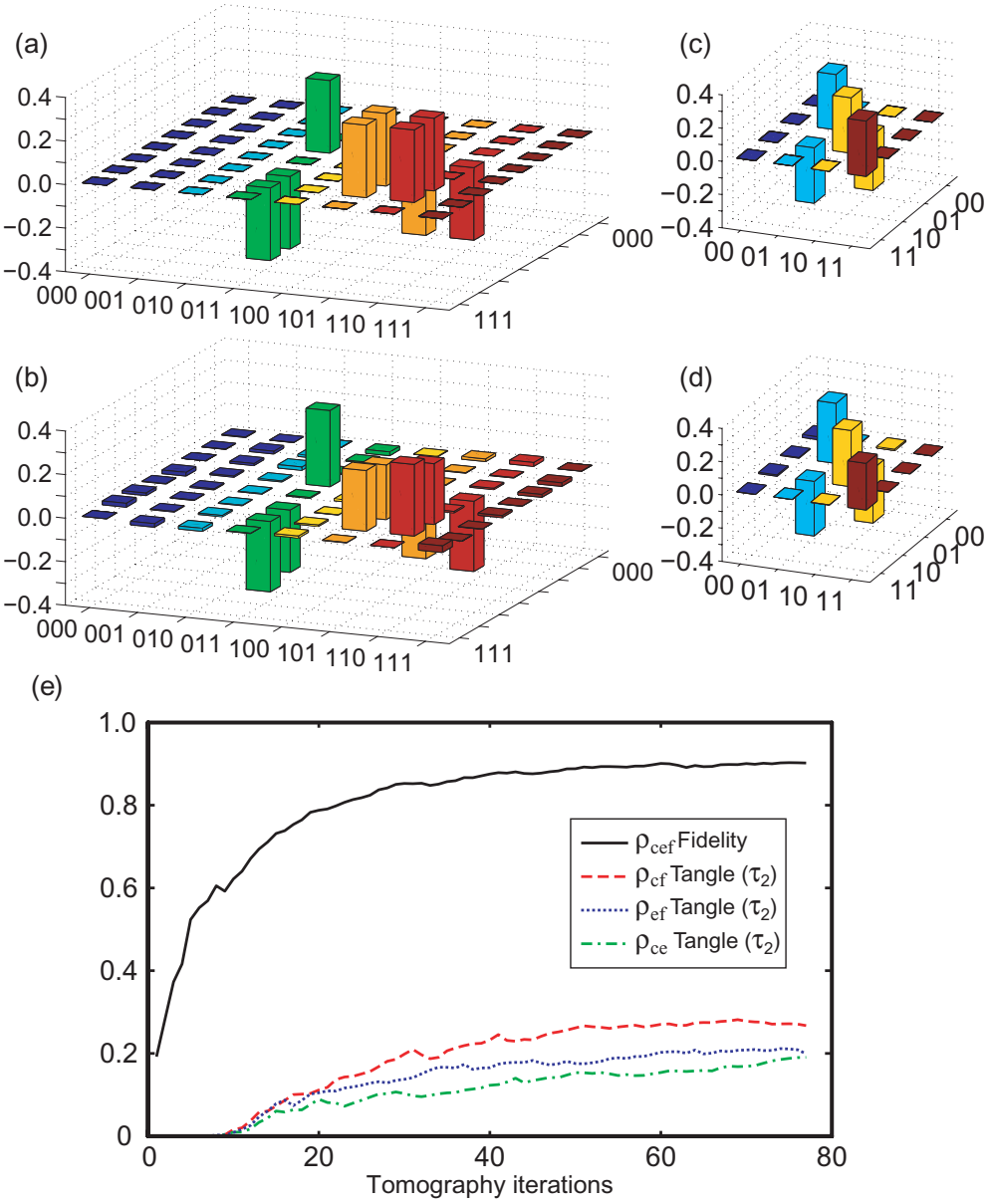

Figure 2. Results for $\theta = \pi/4$ (equation (2)). (a) Ideal and (b) measured three-qubit density matrices. Fidelity $F = 0.90 \pm 0.03$ (with the W state), linear entropy $S_{\mathrm{L}} = 0.20 \pm 0.03$, tripartite negativity $N_3 = 0.80 \pm 0.03$. (c) Ideal and (d) measured reduced state of qubits c and f reconstructed via $\rho_{cf} = \mathrm{Tr}_{\mathrm{e}}(\rho_{cef})$. Fidelity $F = 0.94 \pm 0.02$ (with the MEMS [23, 24]), linear entropy $S_{\mathrm{L}} = 0.61 \pm 0.02$ (ideal 5/9), tangle $\tau_2 = 0.27 \pm 0.03$ (ideal 4/9). (e) Iterative tomography results: we use convex optimization and fixed weight estimation to reconstruct physical density matrices and Monte–Carlo simulations of Poissonian photon-counting fluctuations for error analysis [26]–[28]. We use the following standard definitions: the fidelity between two mixed states is $F(\rho, \sigma) \equiv \mathrm{Tr}[\sqrt{\sqrt{\rho}\sigma\sqrt{\rho}}]^2$; and the linear entropy [20] is $S_{\mathrm{L}}(\rho) \equiv d(1 - \mathrm{Tr}[\rho^2])/(d-1)$, where d is the system dimension.

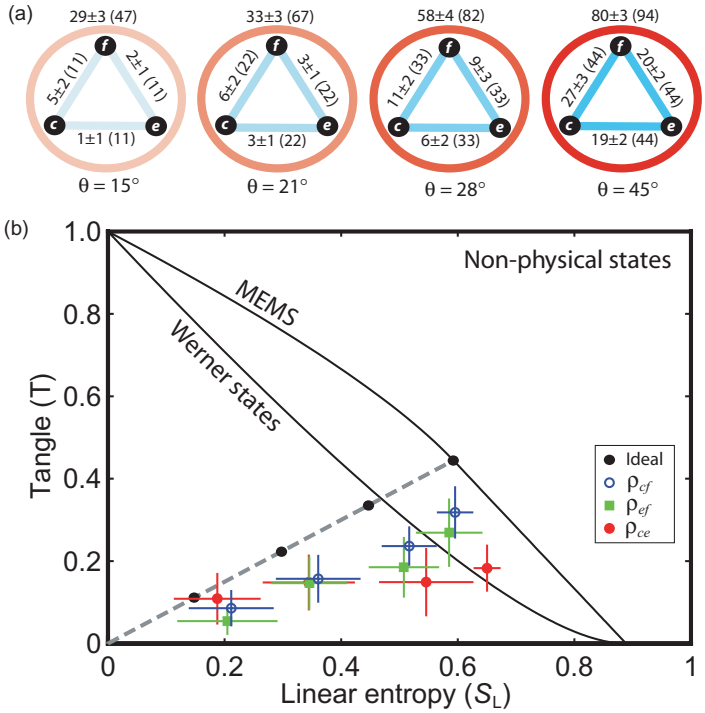

Figure 3. Results for $\theta = \{15^\circ, 21^\circ, 28^\circ, 45^\circ\}$, equation (2). (a) Measured (ideal) entanglement (in %) in three-qubit output states (ρ_{cef}). Black dots are qubits, red circles represent tripartite entanglement (N_3), blue lines represent bipartite (robust) entanglement (τ_2) in reduced states (e.g. line c—e for $\rho_{ce} = \mathrm{Tr}_f\{\rho_{cef}\}$) [14]: high fidelities with ideal configurations, $\{0.90 \pm 0.02, 0.84 \pm 0.03, 0.84 \pm 0.05, 0.90 \pm 0.03\}$, and low linear entropies, $\{0.20 \pm 0.03, 0.22 \pm 0.03, 0.25 \pm 0.03, 0.20 \pm 0.03\}$, respectively. (b) Tangle versus linear entropy plane [23] shows results for reduced two-qubit states measured *directly* by removing the polarization analysis optics of other qubit, and performing two-qubit tomography. The ideal trend (equation (2), dashed), Werner states [30] and MEMS [23, 24] are also shown. The average fidelity with the ideal is 0.97 ± 0.02.

The dashed line shows the path of the ideal reduced states for varying θ (equation (2)); the residual tangle increases linearly with the entropy, with the pure separable state for $\theta = 0$ at the origin, and an MEMS for $\theta = \pi/4$. Due to the symmetry properties of the ideal three-qubit states, this trend does not depend on which qubit is lost. The results show a good correlation with the ideal trend and high fidelities with the expected states (see caption); we can tune the level of robust entanglement in our system.

The reduced entanglement in our results is largely due to optical mode distinguishability caused by alignment drift during the long data runs. The improved bipartite entanglement of figure 3(b) over figure 3(a) reflects a shorter run duration. Another source of error is the higher order emission from SPDC [31]. Both processes introduce extra mixture into the results (there is already mixture in the ideal two-qubit subspaces) and thereby lower the entanglement. The bipartite entanglement is more sensitive to these effects at low θ, because weaker entanglement can be almost completely washed out by extra mixture which would only reduce entanglement

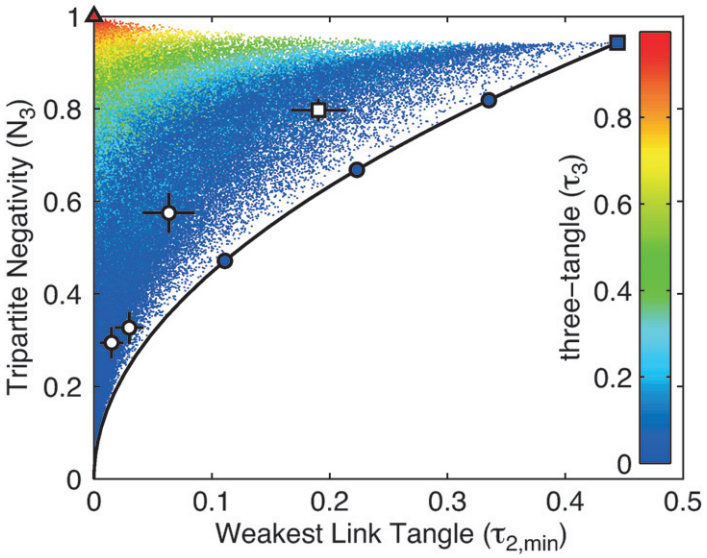

Figure 4. Plot of N_3 versus $\tau_{2,\min}$ (equation (3)) with 300 000 randomly selected pure three-qubit states [34]. Black curve: ideal positions of our states (equation (2)) with $\theta = 0$ (at the origin) to $\pi/4$. The four experimentally measured three-qubit states (white, figure 3(a)) and three-qubit GHZ (red triangle) and W states (blue square) are also shown. The density of states near the boundary (our ideal states) is lower because the set of three-qubit W-class states is of measure zero compared with the set of three-qubit GHZ-class states [4].

in a more strongly entangled state. Important ways to improve entanglement are to increase stability (e.g. by moving to fibre- or micro-optics-based systems [32, 33]) and develop better single photon sources. Beam-splitter reflectivity errors can affect the symmetry of bipartite entanglement. Indeed using our measured values (with deviations $\sim 1\%$) with a simple model predicts that the tangle between qubits c and f will be higher, as observed in our results.

Dür *et al* [4] showed that entanglement in a three-qubit W state is maximally robust in two respects. Firstly, it maximizes the 'weakest link' residual tangle between two-qubit subsystems, namely:

$$\tau_{2,\min}(\Psi_{abc}) = \min\{\tau_2(\rho_{ab}), \tau_2(\rho_{ac}), \tau_2(\rho_{bc})\}, \tag{5}$$

where Ψ_{abc} is any pure three-qubit state and, e.g. $\rho_{ab} = \mathrm{Tr}_c\{\Psi_{abc}\}$. Secondly, it has the highest average residual tangle over the two-qubit subspaces. Figure 4 shows N_3 versus $\tau_{2,\min}$ (equation (3)) for 300 000 pure three-qubit states randomly selected using the Haar measure [34, 35], with the colour scale representing the three-tangle (τ_3). The black line shows the curve for our ideal states (equation (2)), from the separable state at the origin ($\theta = 0$) to the W state ($\theta = \pi/4$), which reaches the maximum possible $\tau_{2,\min}$ value of 4/9. This line clearly represents a boundary in robust configurations of entanglement: for a given level of genuine pure-state three-qubit entanglement (N_3) the weakest bipartite link between any pair of qubits in our ideal states is of optimal strength. States that are not optimal in this sense have at least one weaker bipartite link: there is a 'linchpin' qubit which, if lost, will leave less bipartite entanglement between the remaining qubits. Figure 4 includes the positions of the four measured states shown in figure 3(a). Note that, even though our measured W state has a fidelity

of over 90% with the ideal, the value of $\tau_{2,\min}$ is less than half of the expected value. Clearly maximizing this property is far more experimentally challenging than achieving a high state fidelity. Similar numerical simulations show that our ideal states are not optimal with respect to the average residual entanglement. However, states that improve on ours in this respect do so at the expense of losing a symmetric distribution of entanglement; they always have at least one weaker bipartite link which is less than (or equal to) the weakest link entanglement in our states.

In conclusion, we have demonstrated and fully characterized a new level of control over multipartite entanglement in the laboratory. Our scheme provides tunable control over the level of W-class entanglement between three or more photonic qubits. Furthermore, as we tune the entanglement, it always remains in a highly symmetric configuration that is optimally robust against information loss—a desirable feature in many experimental situations where entanglement is a valuable resource. We predict that the ability to store, generate or transmit entanglement in such low loss configurations will be important in the emerging field of quantum technology.

Acknowledgments

We are thankful to Guifre Vidal and Andrew White for valuable discussions. This work was supported by the Australian Research Council, the DEST Endeavor Europe programs, and an IARPA-funded US Army Research Office Contract. NKL also acknowledges support from the Austrian Science Foundation (FWF), project number SFB 015 P06.

References

[1] Nielsen M A and Chuang I L 2000 *Quantum Computation and Quantum Information* (Cambridge: Cambridge University Press)
[2] Giovannetti V, Lloyd S and Maccone L 2004 *Science* **306** 1330
[3] Raussendorf R and Briegel H J 2001 A one-way quantum computer *Phys. Rev. Lett.* **86** 5188–91
[4] Dür W, Vidal G and Cirac J I 2000 *Phys. Rev.* A **62** 062314
[5] Verstraete F *et al* 2002 *Phys. Rev.* A **65** 052112
[6] Bastin T *et al* 2007 arXiv:0710.3720
[7] Kendon V M, Nemoto K and Munro W J 2002 *J. Mod. Opt.* **49** 1709
[8] Eibl M *et al* 2004 *Phys. Rev. Lett.* **92** 077901
[9] Kiesel N *et al* 2007 *Phys. Rev. Lett.* **98** 063604
[10] Walther P, Resch K J and Zeilinger A 2005 *Phys. Rev. Lett.* **94** 240501
[11] Lu C-Y *et al* 2007 *Nat. Phys.* **3** 91
[12] Bogdanov Y I, Krivitsky L A and Kulik S P 2003 *JETP Lett.* **78** 352
[13] Coffman V, Kundu J and Wootters W K 2000 *Phys. Rev.* A **61** 052306
[14] Sabin C and Garcia-Alcaine G 2007 arXiv:0707.1780
[15] Love P J e 2007 *Quantum Inf. Process.* **6**
[16] Wei T-C *et al* 2003 *Phys. Rev.* A **67** 022110
[17] Hardy L 1993 *Phys. Rev. Lett.* **71** 1665–8
[18] White A G, James D V, Eberhard P H and Kwiat P G 1993 *Phys. Rev. Lett.* **71** 1665–8
[19] Acén A, Richard G and Gisin N 2005 *Phys. Rev. Lett.* **95** 210402
[20] James D F V *et al* 2001 *Phys. Rev.* A **64** 052312
[21] Lanyon B P *et al* 2007 *Phys. Rev. Lett.* **99** 250505
[22] Bourennane M *et al* 2004 *Phys. Rev. Lett.* **92** 087902

[23] Munro W J *et al* 2001 *Phys. Rev.* A **64** 030302
[24] Peters N A *et al* 2004 *Phys. Rev. Lett.* **92** 133601
[25] Ishizaka S and Hiroshima T 2000 *Phys. Rev.* A **62** 022310
[26] O'Brien J L *et al* 2004 *Phys. Rev. Lett.* **93** 080502
[27] de Burgh M, Doherty A and Gilchrist A 2007 in preparation
[28] Langford N K 2007 *PhD Thesis* The University of Queensland, Brisbane, QLD, Australia
[29] Langford N K *et al Phys. Rev. Lett.* **95** 210504
[30] Werner R F 1989 *Phys. Rev.* A **40** 4277
[31] Weinhold T J *et al* 2007 in preparation
[32] Politi A *et al* 2008 *Science* **320** 646
[33] Clark A S *et al* 2008 arXiv:0802.1676
[34] Haar A 1993 *Ann. Math.* **34** 147–69
[35] Nemoto K 2000 *J. Phys. A: Math. Gen.* **33** 3493–506